Available online at www.sciencedirect.com
SCIENCE DIRECT®
PERGAMON
Polyhedron 22 (2003) 53–65
POLYHEDRON
www.elsevier.com/locate/poly

Diorganotin(IV)-promoted deamination of amino acids by pyridoxal: SnR_2^{2+} complexes of pyridoxal 5′-phosphate and of the Schiff base pyridoxal-pyridoxamine (PLPM), and antibacterial activities of PLPM and [SnR_2(PLPM-2H)] (R = Me, Et, Bu, Ph)

José S. Casas [a,*], Alfonso Castiñeiras [a], Félix Condori [a], María D. Couce [b], Umberto Russo [c], Agustín Sánchez [a], Rafael Seoane [d], José Sordo [a,*], José M. Varela [a]

[a] Departamento de Química Inorgánica, Facultade de Farmacia, Universidade de Santiago de Compostela, 15782 Santiago de Compostela, Galicia, Spain
[b] Departamento de Química Inorgánica, Facultade de Ciencias, Universidade de Vigo, 36200 Vigo, Galicia, Spain
[c] Dipartimento di Chimica Inorganica, Metallorganica ed Analitica, Università di Padova, Padua, Italy
[d] Departamento de Microbiología, Facultade de Medicina, Universidade de Santiago de Compostela, 15782 Santiago de Compostela, Galicia, Spain

Received 2 July 2002; accepted 11 September 2002

Abstract

Pyridoxal 5′-phosphate (PLP) and pyridoxal (PL) itself were reacted with diorganotin(IV) derivatives in the presence and absence of aminoacids. With PLP the complexes [SnR_2(PLP-2H)] (R = Me, Et, Bu) were isolated and characterized by EI and FAB mass spectrometry and by IR, Raman and Mössbauer spectroscopy. Reaction mixtures containing PL, valine or glycine and $SnR_2(OAc)_2$ (R = Me, Et) afforded complexes of the form [SnR_2(PLPM-2H)], where PLPM is the Schiff base formed by condensation of PL and pyridoxamine (PM). PM was presumably formed by transamination between valine or glycine and PL. The PLPM complexes, and their butyl and phenyl analogues, were also synthesized directly by reacting SnR_2O and PLPM, and were characterized by EI and FAB MS, by IR, Raman, Mössbauer and NMR spectroscopy, and in the case of the methyl and ethyl compounds by single-crystal X-ray diffractometry. Crystals of [$SnMe_2$(PLPM-2H)]·H_2O and [$SnEt_2$(PLPM-2H)] consist of molecules in which the ligand is bound to the metal through the O atoms of the two deprotonated phenolic hydroxyl groups and the iminic N atom, and the metal exhibits distorted square pyramidal coordination. Both PLPM and its complexes show intense antibacterial activity against *Pseudomonas aeruginosa* (ATCC27853), but only the complexes exhibit significant activity against the other four bacterial strains assayed, *Staphylococcus aureus*, *Bacillus subtilis*, *Escherichia coli* and a carbapenem-resistant *P. aeruginosa* strain.

Keywords: Deamination of amino acids; Diorganotin(IV) complexes; Pyridoxal 5′-phospate; Pyridoxal–pyridoxamine Schiff base; X-ray structures; Antibacterial activity

1. Introduction

Pyridoxal 5′-phosphate (PLP, Scheme 1), the biologically active form of vitamin B_6 (PL, PM or PN, Scheme 1), acts as coenzyme in several biosynthetic, metabolic or regulatory processes.

Among the processes most widely known [1] which involve the synthesis, degradation and interconversion of the amino acids (aa), particular attention has been paid to the elimination of the aa α-amino groups (the first step in the catabolism of most L-aminoacids), which is catalysed by aminotransferases [1]. This reaction begins with the PLP cofactor and the sustrate (aa) forming a Schiff base (the external aldimine of Scheme 2), and in the following step the C_α H-atom is heterolytically removed, giving a quinonoid intermediate that evolves to the ketimine form upon the capture of a proton.

Although PLP dependent enzymes seem not to use metal ions as additional cofactors, it was soon observed

* Corresponding author
E-mail addresses: qiscasas@usc.es (J.S. Casas), qijsordo@usc.es (J. Sordo).

0277-5387/02/$ - see front matter
PII: S0277-5387(02)01331-1

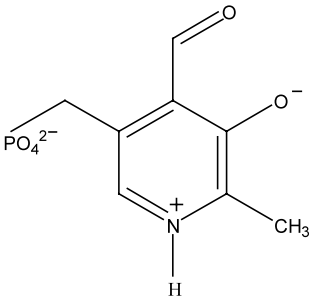

PLP

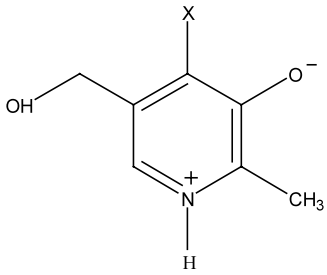

Pyridoxal, PL (X = -CHO)

Pyridoxamine, PM (X = $-CH_2NH_2$)

Pyridoxine, PN (X = $-CH_2OH$)

Scheme 1.

[2] that metal ions can promote many of the nonenzymatic reactions of PLP, which led to several studies on the coordination schemes and structural parameters of metal complexes of PLP–aa [3] and PL–aa [4] Schiff bases. Although it was originally assumed that the metal ion is more effective than a proton for stabilizing the quinonoid intermediate, its influence seems rather to be due to its promoting the formation of the Schiff base [2].

In continuation of our previous work on the interaction of organotin(IV) compounds with vitamins and their derivatives [5], we have studied the systems PLP/SnR_2^{2+} and PL/SnR_2^{2+} in the absence and presence of aa, and in the latter case have explored the influence of the organometallic ions on transamination reactions. Since the organotin complexes of Schiff bases [6] and pyridoxal (PL) derivatives [7] often have significant antibacterial activity, some of the compounds prepared were tested against Gram-positive and Gram-negative bacteria.

2. Experimental

2.1. Material and methods

Pyridoxal 5-phosphate (Sigma), pyridoxal hydrochloride (Sigma), pyridoxamine dihydrochloride (Sigma), dimethyltin oxide (Alfa) and dibutyltin oxide (Aldrich) were used as received. Diethyl- and diphenyltin oxides were obtained by treating the corresponding chlorides with sodium hydroxide [8]. PL [9] and pyridoxamine (PM) [10] were prepared from the hydrochlorides by reacting them with KOH. The Schiff base pyridoxal–pyridoxamine (PLPM) was prepared by adding 0.34 g (2 mmol) of solid PM to a stirred solution of 0.33 g (2 mmol) of PL in toluene–ethanol (80:20 v/v, 100 ml), refluxing for 5 h, and evaporating the solvents to obtain a yellow solid that was vacuum dried. Yield 98%. Melting point (m.p.) > 250 °C. Found: C, 60.7; N, 13.3; H, 6.4. PLPM requires: C, 60.6; N, 13.2; H,

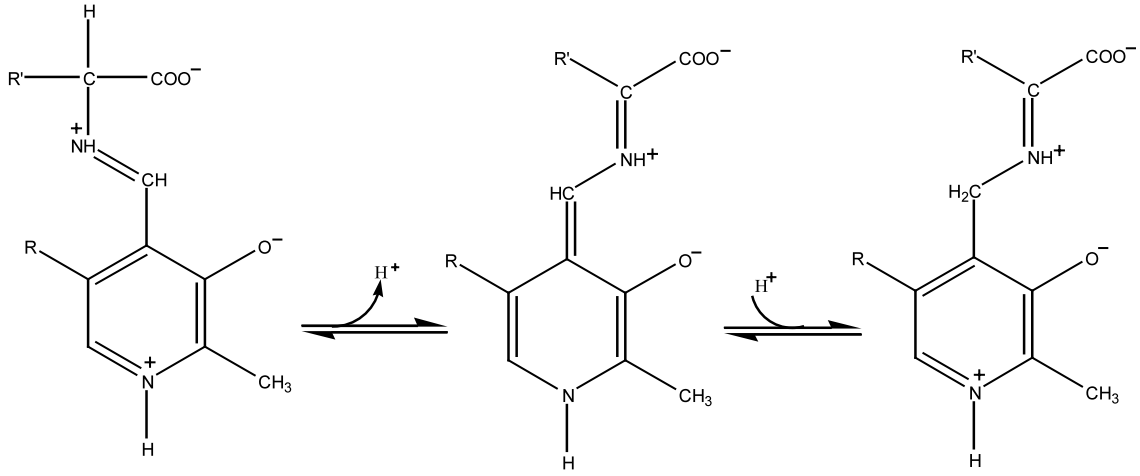

Schiff base
(External aldimine)

Quinonoid

Ketimine

Scheme 2.

6.0%. Infrared and Raman (in parentheses), cm^{-1}: 3348m, 3172s,br, ν(OH); 1635s (1634vs), ν(C–N); 1587sh (1590sh), ν(ring); 1285s (1286 m), $\nu(C-O_{phenolic})$; 1031s (1031w), $\nu(C-O_{hydroxymethyl})$. ^{13}C CP MAS (see Fig. 1 for numbering scheme): δ[C(29)] 163.7; δ[C(23)] 154.9; δ[C(13)] 151.2; δ[C(15)] 151.2; δ[C(25)] 146.5; δ[C(26)] 140.8; δ[C(16)] 137.0; δ[C(22)] 132.2; δ[C(12)] 132.2; δ[C(24)] 131.0; δ[C(14)] 120.6; δ[C(27)] 59.3; δ[C(17)] 57.8; δ[C(19)] 54.8; δ[C(210)] 17.6; δ[C(110)] 16.3. NMR data in dmso-d_6. ^1H: δ[N(21)H] 14.26s(1); δ[C(29)H] 9.01s(1); δ[C(26)H] 7.96s(1); δ[C(16)H] 7.86s(1); δ[O(23)H] 5.34s,br(1); δ[O(13)H] 5.22s,br(1); $\delta[C(19)H_2]$ 4.93s(2); $\delta[C(27)H_2]$ 4.63s(2); $\delta[C(17)H_2]$ 4.57s(2); $\delta[C(210)H_3]$ 2.39s(3); $\delta[C(110)H_3]$ 2.31s(3). ^{13}C: δ[C(29)] 164.3; δ[C(23)] 154.3; δ[C(13)] 149.4; δ[C(15)] 148.4; δ[C(25)] 146.2; δ[C(26)] 139.7; δ[C(16)] 137.0; δ[C(22)] 134.0; δ[C(12)] 132.7; δ[C(24)] 129.8; δ[C(14)] 118.9; δ[C(27)] 58.9; δ[C(17)] 58.3; δ[C(19)] 52.4; δ[C(210)] 19.8; δ[C(110)] 18.6.

Elemental analysis was performed with a Fisons 1108 microanalyser. Melting points were determined with a Büchi apparatus and are uncorrected. Mass spectra were recorded on a Kratos MS50TC spectrometer connected to a DS90 system and operating under either EI conditions (direct insertion probe, 70 eV, 250 °C) or in FAB mode (*m*-nitrobenzyl alcohol, Xe, 8 eV; ca. 1.28×10^{-15} J); ions were identified by DS90 software and the intensities of the metallated peaks were calculated using the isotope ^{120}Sn. IR spectra (from KBr pellets or Nujol mulls) and Raman spectra (from polycrystalline samples) were recorded on a Bruker IFS66V FT IR spectrometer equipped with an FRA-106 Raman accessory, and are reported in the synthesis section using the following abbreviations: vs, very strong; s, strong; m, medium; w, weak; sh, shoulder; br, broad. Mössbauer spectra were recorded at 80.0 K in a Harwell cryostat; the $Ca^{119m}SnO_3$ source (15 mCi, NEN) was kept at room temperature and moved with a triangular velocity wave form, and appropriate computer programs were employed to fit Lorentzian lineshapes to the experimental data. Solid-state NMR spectra were recorded on a Bruker AMX 300 spectrometer at 75.40 MHz using 7 mm o.d. zirconia rotors spinning at 3 or 4 kHz and the standard Bruker CPTOSS or CP_2LEV pulse programs, with a contact time of 1 ms and a recycle delay of 5 s (linewidths varied between 100 and 300 Hz); chemical shifts are referred to glycine (δ 176.3 ppm). ^1H and ^{13}C NMR spectra in solution were recorded at r.t. on a Bruker AMX 300 spectrometer operating at 300.14 and 75.40 MHz, respectively, using 5 mm o.d. tubes; chemical shifts are reported relative to TMS using the solvent signal (δ $^1H = 2.50$ ppm; δ $^{13}C = 39.5$ ppm) as reference. ^{119}Sn NMR spectra were recorded at 186.50 MHz on a Bruker AMX 500 spectrometer using 5 mm o.d. tubes and are reported relative to external neat $SnMe_4$ (δ ^{119} Sn = 0 ppm). The conductivities of 10^{-3} M solutions in dmf were measured in a Crison MicroCM2202 conductivity meter.

Antibacterial activity was assayed against five bacterial strains, two of them Gram-(+) [*Staphylococcus aureus* (ATCC29213) and *Bacillus subtilis* (ATCC6633)] and three Gram-(−) [*Escherichia coli* (ATCC25922), *Pseudomonas aeruginosa* (ATCC27853) and a clinical isolate of *P. aeruginosa* characterized by its resistance to antibacterial carbapenems]. Antibacterial activity was initially assayed by Muller–Hinton agar diffusion methods. Discs of paper 5 mm in diameter were loaded with 20 μl of a 2 μg ml^{-1} solution of the product to be tested in 9:1 ethanol–water; control discs were loaded with solvent alone. The discs were placed on dishes of Muller–Hinton agar inoculated with the appropriate bacterium and after 24 h incubation at 37 °C the diameter of the zone of bacterial growth inhibition was measured. Minimum inhibitory concentrations (MICs) for those which showed activity in the diffusion test were determined using serial dilutions in Muller–Hinton broth in microwell plates (200 μl of culture per well).

Elemental analyses, mass, IR, Raman and NMR spectra and X-ray data were obtained at CACTUS, University of Santiago de Compostela, Galicia, Spain.

2.2. Synthesis of complexes

2.2.1. [$SnMe_2$(PLP-2H)] (**1**)

2.2.1.1. Method A. To 0.25 g (1 mmol) of PLP in 25 ml of 3:1 methanol–water was added 0.12 g (1 mmol) of valine, giving a yellow solution. Addition of 0.27 g (1 mmol) of $SnMe_2(OAc)_2$ immediately afforded a yellow solid that after 12 h stirring was filtered out, washed with absolute methanol and vacuum dried. Yield 89%. M.p. > 250 °C. Found: C, 28.3; N, 3.7; H, 3.4. $[SnMe_2(PLP\text{-}2H)]\cdot 1.5H_2O$ requires: C, 28.6; N, 3.8; H, 3.3%.

2.2.1.2. Method B. Solid dimethyltin(IV) oxide (0.33 g, 2 mmol) was added to 0.49 g (2 mmol) of PLP dissolved in toluene–ethanol (80:20 v/v, 100 ml). After 10 h refluxing, the water was removed by azeotropic distillation in a Dean–Stark funnel and the yellow solid formed was filtered out and vacuum dried. Yield 95%. M.p. > 250 °C. Found: C, 30.4; N, 3.2; H, 3.4. [$SnMe_2$(PLP-2H)] requires: C, 30.4; N, 3.6; H, 3.6%. The main metallated signals in the EI spectrum are at *m/e* (ion, intensity) 165 ([PL-2H], 100), 149 ([$SnMe_2$-H], 32.9), 136 ([SnMe+H], 56.0) and 120 ([Sn], 17.9); the FAB spectrum shows the same metallated signals. Infrared and Raman (in parentheses), cm^{-1}: 1109vs, 1043s (1030w), 1002s (1002m), $\nu(PO_3^{2-})$; 580sh (583w), ν_{asym}(Sn–C); 521m,br (529vs), ν_{sym}(Sn–C). Mössbauer: I.S. 1.18, Q.S. 3.80, Γ 0.92 mms^{-1}, $A_{2/1}$ 1.06.

*2.2.2. [SnEt$_2$(PLP-2H)] (**2**)*

PLP (0.49 g, 2 mmol) was dissolved in toluene–ethanol (80:20 v/v, 100 ml), and solid diethyltin(IV) oxide (0.39 g, 2 mmol) was added. After 10 h refluxing, water was removed by azeotropic distillation in a Dean–Stark funnel and the yellow solid formed was filtered out and vacuum dried. Yield 95%. M.p. > 250 °C. Found: C, 33.5; N, 3.0; H, 4.5. [SnEt$_2$(PLP-2H)]·0.5H$_2$O requires: C, 34.0; N, 3.3; H, 4.3%. The main metallated signal in the EI spectrum is at *m/e* (ion, intensity) 120 ([Sn], 10.5). The EI spectrum also shows signals for the pyridine ring and its fragments, and the FAB spectrum signals at 176 ([SnEt$_2$-2H], 3.4) and 135 ([SnMe], 4.4). Infrared and Raman (in parentheses), cm^{-1}: 1103vs,b (1105w), 1009vs, ν(PO$_3^{2-}$); 545w (541w), ν_{asym}(Sn–C); 500w (500vs), ν_{sym}(Sn–C). Mössbauer: I.S. 1.28, Q.S. 3.50, Γ 0.92 mm s^{-1}, $A_{2/1}$ 1.00.

*2.2.3. [SnBu$_2$(PLP-2H)] (**3**)*

PLP (0.49 g, 2 mmol) was dissolved in toluene–ethanol (80:20 v/v, 100 ml), and solid dibutyltin(IV) oxide (0.49 g, 2 mmol) was added. After 10 h refluxing water was removed by azeotropic distillation in a Dean–Stark funnel and the yellow solid formed was filtered out and vacuum dried. Yield 95%. M.p. > 250 °C. Found: C, 40.1; N, 2.9; H, 5.4. [SnBu$_2$(PLP-2H)] requires: C, 40.1; N, 2.9; H, 5.5%. The main metallated signals in the EI spectrum are at m/e (ion, intensity): 149 ([SnMe$_2$-H], 83), 136 ([SnMe+H], 58) and 120 ([Sn], 39). The EI spectrum also shows signals at *m/e* 247 ([PLP], 12) and 165 ([PL-2H], 100) and others for the pyridine ring and its fragments, and the FAB spectrum signals at 958 ([SnBu$_2$(PLP-2H)]$_2$, 13.0), 872 ([(SnBu$_2$(PLP-2H))$_2$–C$_6$H$_{14}$], 13.4), 850 ([(Sn$_2$Bu$_2$PLP$_2$+2H)], 4.24), 464 ([SnBu$_2$(PLP-2H)–CH$_3$], 14.4), 329 ([SnBu$_2$O$_4$P], 14.3) and 177 ([SnBu], 21.7). Infrared and Raman (in parentheses), cm^{-1}: 1127vs, 1078m (1079w), 1003vs (1001w), ν(PO$_3^{2-}$). Mössbauer: I.S. 1.16, Q.S. 3.31, Γ 0.89 mm s^{-1}, $A_{2/1}$ 1.04.

*2.2.4. [SnMe$_2$(PLPM-2H)] (**4**)*

2.2.4.1. Method A. To a solution of SnMe$_2$Cl$_2$ (0.44 g, 2 mmol) in methanol–water (80:20 v/v, 20 ml) was added 0.66 g (4 mmol) of solid Ag(OAc), and the AgCl formed after 6 h stirring was filtered out to leave Solution A. To a solution of valine (0.47 g, 4 mmol) in the same solvent (20 ml) were added solid NaOH (0.16 g, 4 mmol) and solid PL (0.67 g, 4 mmol), and the mixture so obtained was stirred for 5 h to obtain Solution B. Finally, Solution B was added with stirring to Solution A and stirring was continued for 1 day, after which the solution was concentrated and the yellow solid formed was filtered out and dried in vacuo. Yield 60%. M.p. > 250 °C. Found: C, 44.5; N, 8.4; H, 5.0. [SnMe$_2$(PLPM–2H)]·H$_2$O requires: C, 44.8; N, 8.7; H, 5.2%. The main metallated signals in the EI spectrum are at m/e (ion, intensity) 465 ([SnMe$_2$(PLPM-2H)], 32.4), 450 ([SnMe$_2$(PLPM-2H)–CH$_3$], 75.8), 435 ([SnMe$_2$(PLPM-2H)–2CH$_3$], 25.4), 150 ([SnMe$_2$], 28.8), 135 ([SnMe], 100) and 120 ([Sn], 78.8). The EI spectrum also shows signals for the pyridine ring and its fragments, and the FAB spectrum a signal at 314 ([SnMe$_2$(PM)], 17.4). Infrared and Raman (in parentheses), cm^{-1}: 3266s,br, ν(OH); 1628vs (1630vs), ν(C=N); 1581w (1582w), ν(ring); 1321m, 1290m, ν(C–O$_{phenolic}$); 1027s, 1020s (1030w, 1020w), ν(C–O$_{hydroxymethyl}$); 549w (547w), ν_{asym}(Sn–C); 514m (519vs), ν_{sym}(Sn–C). Mössbauer: I.S. 1.45, Q.S. 3.64, Γ 0.87 mms^{-1}, $A_{2/1}$ 1.11. ^{13}C CP MAS: δ[C(29)] 166.1; δ[C(23)] 159.6; δ[C(13)] 158.2; δ[C(15)] 151.3; δ[C(25)] 151.3; δ[C(26)] 135.5; δ[C(16)] 135.5; δ[C(22)] 132.4; δ[C(12)] 132.4; δ[C(24)] 129.2; δ[C(14)] 117.8; δ[C(27)] 60.6; δ[C(17)] 60.6; δ[C(19)] 60.6; δ[C(210)] 18.1; δ[C(110)] 17.0; δ[C–Sn] 11.4, 7.0. NMR data in dmso-d_6. ^{1}H: δ[C(29)H] 8.93s(1); $^3J(^1H-^{119}Sn) = 26.0$ Hz; δ[C(26)H] 7.60s(1); δ[C(16)H] 7.57s(1); δ[O(23)H] 5.50t(1); δ[O(13)H] 5.17t(1); δ[C(19)H$_2$] 4.89s(2); δ[C(27)H$_2$] 4.54s(2); $^3J = 5.3$ Hz; δ[C(17)H$_2$] 4.52s(2); $^3J = 5.3$ Hz; δ[C(210)H$_3$] and δ[C(110)H$_3$] 2.25s(6); δ[CH$_3$–Sn] 0.50s(6); $^2J(^1H-^{119/117}Sn) = 95.9$ Hz. ^{13}C: δ[C(29)] 169.6; δ[C(23)] 160.1; δ[C(13)] 156.6; δ[C(15)] 153.9; δ[C(25)] 149.1; δ[C(26)] 135.7; δ[C(16)] 134.1; δ[C(22)] 131.1; δ[C(12)] 132.2; δ[C(24)] 131.4; δ[C(14)] 117.9; δ[C(27)] 59.3; δ[C(17)] 58.6; δ[C(19)] 57.3; δ[C(210)] 19.8; δ[C(110)] 19.4; δ[C–Sn] 5.8; $^1J(^{13}C-^{119/117}Sn) = 910.4/869.6$ Hz. ^{119}Sn: δ −305.9. Λ_M (dmf), 25.7 S cm^2 mol^{-1}. Crystals appropriate for the X-ray diffractometry were obtained by crystallization in absolute methanol.

2.2.4.2. Method B. To 0.63 g (2 mmol) of PLPM in toluene–ethanol (80:20 v/v, 100 ml) was added solid SnMe$_2$O (0.33 g, 2 mmol). After 8 h refluxing, water was removed by azeotropic distillation in a Dean–Stark funnel. The resulting solution was concentrated, and the yellow solid formed was filtered out and vacuum dried. Yield 75%. M.p. > 250 °C. Found: C, 46.9; N, 8.9; H, 4.8. [SnMe$_2$(PLPM-2H)] requires: C, 46.5; N, 9.0; H, 4.9%.

*2.2.5. [SnEt$_2$(PLPM-2H)] (**5**)*

To a solution of SnEt$_2$Cl$_2$ (0.50 g, 2 mmol) in methanol–water (80:20 v/v, 20 ml) was added solid Ag(OAc) (0.66 g, 4 mmol), and the AgCl formed after 6 h stirring was filtered out to leave Solution A. To a solution of valine (0.47 g, 4 mmol) in the same solvent (20 ml) were added solid NaOH (0.16 g, 4 mmol) and solid PL (0.67 g, 4 mmol), and this mixture was stirred for 5 h to obtain Solution B. Solution B was added with stirring to Solution A and stirring was continued for 1 day, after which the solution was concentrated and the yellow solid formed was filtered out and dried in vacuo.

Yield 62%. M.p. > 250 °C. Found: C, 48.6; N, 8.5; H, 5.6. [$SnEt_2$(PLPM-2H)] requires: C, 48.9; N, 8.5; H, 5.5%. The main metallated signals in the EI spectrum are at *m/e* (ion, intensity) 493 ([$SnEt_2$(PLPM-2H)], 6.8), 463 ([$SnEt_2$(PLPM-2CH_3)], 81.6), 435 ([$SnEt_2$(PLPM-2CH_2–CH3)], 39.3), 149 ([$SnEt_2$], 45.7), 135 ([SnMe], 84.4) and 120 ([Sn], 70.5). The EI spectrum also shows signals for the pyridine ring and its fragments, and the FAB spectrum signals at 179 ([$SnEt_2$], 3.2) and 163 ([$SnEt_2$–CH_2], 3.6). Infrared and Raman (in parentheses), cm^{-1}: 3286m, 3139m,br, ν(OH); 1633vs (1634vs), ν(C–N); 1578w (1576w), ν(ring); 1313m, 1287m, ν(C–$O_{phenolic}$); 517w (518w), ν_{asym}(Sn–C); 480w (487vs), ν_{sym}(Sn–C). Mössbauer: I.S. 1.54, Q.S. 3.63, Γ 0.88 mms^{-1}, $A_{2/1}$ 0.97. ^{13}C CP MAS: δ[C(29)] 169.5; δ[C(23)] 160.1; δ[C(13)] 155.4; δ[C(15)] 149.7; δ[C(25)] 149.7; δ[C(26)] 137.7; δ[C(16)] 134.6; δ[C(22)] 132.2; δ[C(12)] 132.2; δ[C(24)] 130.0; δ[C(14)] 120.3; δ[C(27)] 59.1; δ[C(17)] 59.1; δ[C(19)] 55.7; δ[C(210)] 18.6; δ[C(110)] 16.9; δ[C(α)–Sn] 22.9; δ[C(β)–Sn] 11.4, 9.8. NMR data in dmso-d_6. ^{1}H: δ[C(29)H] 8.98s(1); $^3J(^1H–^{119}Sn) = 25.0$ Hz; δ[C(26)H] 7.59s(1); δ[C(16)H] 7.54s(1); δ[O(23)H] 5.23t(1); $^3J = 5.4$ Hz, δ[O(13)H] 5.16t(1); $^3J = 5.4$ Hz; δ[C(19)H_2] 4.88s(2); δ[C(27)H_2] 4.53d(2); $^3J = 5.2$ Hz; δ[C(17)H_2] 4.50s(2); $^3J = 5.2$ Hz; δ[C(210)H_3] 2.28s(3); δ[C(110)H_3] 2.26s(3); δ[CH(α)–Sn] 1.23q(4); δ[CH(β)–Sn] 1.02t(6); $^3J(^1H–^{119}Sn) =$ 145.0 Hz. ^{13}C: δ[C(29)] 169.9; δ[C(23)] 160.4; δ[C(13)] 157.3; δ[C(15)] 153.8; δ[C(25)] 148.7; δ[C(26)] 135.4; δ[C(16)] 134.1; δ[C(22)] 132.7; δ[C(12)] 132.3; δ[C(24)] 130.6; δ[C(14)] 117.4; δ[C(27)] 59.3; δ[C(17)] 58.6; δ[C(19)] 57.7; δ[C(210)] 19.7; δ[C(110)] 19.4; δ[C(α)–Sn] 18.7; δ[C(β)–Sn] 10.0.^{119}Sn: δ −326.2, −330.2. Λ_M (dmf), 24.3 S cm^2 mol^{-1}. Crystals suitable for X-ray diffractometry were obtained by crystallization in absolute methanol.

2.2.6. [$SnBu_2$(PLPM-2H)] (**6**)

The Schiff base PLPM (0.63 g, 2 mmol) was dissolved in toluene–ethanol (80:20 v/v, 100 ml), and solid dibutyltin(IV) oxide (0.49 g, 2 mmol) was added. After 8 h refluxing, water was removed by azeotropic distillation in a Dean–Stark funnel, the residual yellow solution was concentrated to dryness, and the oil so obtained was treated with petroleum ether. After 10 h stirring the yellow solid formed was filtered out and dried in vacuo. Yield 90%. M.p. = 75 °C. Found: C, 51.9; N, 8.2; H, 6.1. [$SnBu_2$(PLPM-2H)] requires: C, 52.6; N, 7.7; H, 6.4%. The main metallated signals in the EI spectrum are at *m/e* (ion, intensity) 492 ([$SnBu_2$(PLPM-2H)], 100), 435 ([Sn(PLPM-2H)], 24.2), 236 ([$SnBu_2$H)], 8.8) and 120 ([Sn], 43.8). The EI spectrum also shows signals for the pyridine ring and its fragments, and the FAB spectrum signals at 548 ([$SnBu_2$(PLPM-2H)], 3.6) and 177 ([SnBu)], 7.6). Infrared and Raman (in parentheses), cm^{-1}: 3300m,br, 3196m,br, ν(OH); 1619vs (1620vs), ν(C–N); 1580w (1582w), ν(ring); 1294m (1294m), ν(C–$O_{phenolic}$); 1022m,br, ν(Sn–$O_{hydroxymethyl}$). Mössbauer: I.S. 1.38, Q.S. 2.87, Γ 0.96 mms^{-1}, $A_{2/1}$ 1.07. NMR data in dmso-d_6. ^{1}H: δ[C(29)H] 9.02s(1); $^3J(^1H–^{119}Sn) = 36$ Hz; δ[C(26)H] 7.62s(1); δ[C(16)H] 7.59s(1); δ[O(23)H] 5.25t(1); δ[O(13)H] 5.18t(1); δ[C(19)H_2] 4.94s(2); δ[C(27)H_2] 4.55d(2); $^3J = 5.2$ Hz; δ[C(17)H_2] 4.51s(2); $^3J = 5.3$ Hz; δ[C(210)H_3] 2.27s(3); δ[C(110)H_3] 2.26s(3); δ[CH(α)–Sn] 1.29m(4); δ[CH(β)–Sn] 1.46q(4); $^3J(^1H–^{119}Sn) = 99.0$ Hz; δ[CH(γ)–Sn] 1.23m(4); δ[CH(δ)–Sn] 0.76t(6). ^{13}C: δ[C(29)] 171.3; δ[C(23)] 160.2; δ[C(13)] 156.8; δ[C(15)] 153.7; δ[C(25)] 148.6; δ[C(26)] 135.7; δ[C(16)] 134.2; δ[C(22)] 133.2; δ[C(12)] 132.3; δ[C(24)] 130.7; δ[C(14)] 117.3; δ[C(27)] 59.3; δ[C(17)] 58.5; δ[C(19)] 58.3; δC(210)] 19.4; δ[C(110)] 19.0; δ[C(α)–Sn] 23.6; δ[C(β)–Sn] 27.0; δ[C(γ)–Sn] 26.1; δ[C(δ)–Sn] 13.4.^{119}Sn: δ −285.0. Λ_M (dmf), 22.4 S cm^2 mol^{-1}.

2.2.7. [$SnPh_2$(PLPM-2H)] (**7**)

The Schiff base PLPM (0.63 g, 2 mmol) was dissolved in toluene-ethanol (80:20 v/v, 100 ml), and solid diphenyltin(IV) oxide (0.58 g, 2 mmol) was added. After 8 h refluxing water was removed by azeotropic distillation in a Dean–Stark funnel, the yellow solution was concentrated to dryness, and the yellow solid formed was dried in vacuo. Yield 90%. M.p. > 250 °C. Found: C, 57.6; N, 6.9; H, 5.1. [$SnPh_2$(PLPM-2H)] requires: C, 57.1; N, 7.1; H, 4.6%. The main metallated signal in the EI spectrum is at *m/e* (ion, intensity) 362 ([$SnPh_2$(PM)], 50.7). The EI spectrum also shows signals for the pyridine ring and its fragments, and the FAB spectrum signals at 588 ([$SnPh_2$(PLPM-2H)], 100), 510 ([SnPh(PLPM-2H)], 12.2), 437 ([$SnPh_2$(PM)],18.3), 434 ([Sn(PLPM)], 18.4), 273 ([$SnPh_2$], 5.01), 195 ([SnPh], 20.6) and 120 ([Sn], 21.1). Infrared and Raman (in parentheses), cm^{-1}: 3182m,br, ν(OH); 1620s (1621m), ν(C–N); 1580w (1579w), ν(ring); 1313m (1323m), 1294m (1296), ν(C–$O_{phenolic}$); 1023m (1023m), ν(C–$O_{hydroxyphenyl}$). Mössbauer: I.S. 1.17, Q.S. 2.58, Γ 0.88 mms^{-1}, $A_{2/1}$ 1.00. NMR data in dmso-d_6. ^{1}H: δ[C(29)H] 8.94s(1); $^3J(^1H–^{119}Sn) = 52.0$ Hz; δ[C(26)H] 7.67s(1); δ[C(16)H] not observed; δ[O(23)H] 5.29t(1), $^3J = 5.2$ Hz; δ[O(13)H] 5.14t(1); $^3J = 5.2$ Hz; δ[C(19)H_2] 4.86s(2); $^3J(^1H–^{119}Sn) = 30.7$ Hz; δ[C(27)H_2] 4.59d(2); $^3J = 5.0$ Hz; δ[C(17)H_2] 4.52s(2); $^3J = 5.0$ Hz; δ[C(210)H_3] 2.44s(3); δ[C(110)H_3] 2.37s(3); δ[CH($_o$)–Sn] 7.74d(4); $^3J(^1H–^{119}Sn) = 68.0$ Hz; δ[CH($_{m,p}$)–Sn] 7.28q(8). ^{13}C: δ[C(29)] 167.7; δ[C(23)] 159.7; δ[C(13)] 157.0; δ[C(15)] 153.6; δ[C(25)] 149.3; δ[C(26)] 136.2; δ[C(16)] 135.0; δ[C(22)] 134.1; δ[C(12)] 132.3; δ[C(24)] 130.2; δ[C(14)] 118.5; δ[C(27)] 59.2; δ[C(17)] 58.6; δ[C(19)] 57.6; δ[C(210)] 20.0; δ[C(110)] 19.8; δ[C($_i$)–Sn] 150; δ[C($_o$)–Sn] 135.0; δ[C($_m$)–Sn] 127.9; δ[C($_p$)–Sn] 128.1.^{119}Sn: δ −485.8. Λ_M (dmf), 22.4 S cm^2 mol^{-1}.

2.3. Crystal structure determination

2.3.1. X-ray data collection and reduction

Suitable single crystals were mounted for data collection in Enraf–Nonius CAD4 [11] and MACH3 automatic diffractometers. Data were collected at 293 K using Cu Kα or Mo Kα radiation ($\lambda = 1.54184$ or 0.71073Å) and were corrected for Lorentz and polarization effects [12].

2.3.2. Structure solution and refinement

The structure was solved by direct methods [13] and subsequent Fourier maps, and refined on F^2 by a full-matrix least-squares procedure using anisotropic displacement parameters [14,15]. All hydrogen atoms were located from difference Fourier maps, placed at calculated positions (C–H ·0.93–0.97 Å) and refined isotropically using a riding model. Absolute configuration was established by successful refinement of the Flack [16] parameter. Atomic scattering factors were taken from International Tables for X-ray Crystallography [17]. Molecular graphics were generated with PLATON [18]. The crystal data, experimental details and refinement results are summarized in Table 1.

Table 1
Crystal, data collection and structure refinement parameters

	[$SnMe_2$(PLPM-2H)]·H_2O (**4**·H_2O)	[$SnEt_2$(PLPM-2H)] (**5**)
Empirical Formula	$C_{18}H_{25}N_3O_5Sn$	$C_{20}H_{27}N_3O_4Sn$
Formula weight	482.10	492.14
Wavelength, (Å)	1.54184	0.71073
Crystal system	monoclinic	monoclinic
Space group	*P*2(1) (no. 4)	*C*2/*c* (no. 15)
Unit cell dimensions		
a (Å)	8.6075(5)	12.844(5)
b (Å)	13.3977(6)	12.4708(13)
c (Å)	8.6360(3)	26.022(3)
β (°)	97.579(5)	103.484(19)
V (Å^3)	987.21(8)	4053.3(17)
Z	2	8
D_{calc}, (Mg m^{-3})	1.622	1.613
F(000)	488	2000
μ, (mm^{-1})	10.590	1.292
Crystal size (mm)	0.25 × 0.20 × 0.15	0.35 × 0.20 × 0.20
θ range for data collection, (°)	5.17–75.93	2.31–30.40
Index ranges	$-10 \le h \le 10$; $0 \le k \le 16$; $-10 \le l \le 0$	$-18 \le h \le 17$; $0 \le k \le 17$; $0 \le l \le 37$
Reflections collected	2287	6249
Unique reflections	2149 [$R_{int} = 0.0259$]	6124 [$R_{int} = 0.0531$]
Absorption correction	Psi-scan	Psi-scan
Max/min transmission	0.978, 0.642	0.968, 0.930
Data, restrainst, parameters	2149, 1, 249	6124, 0, 301
Goodness of fit on F^2	1.072	0.971
Final *R* indices [$I > 2\sigma(I)$]	$R_1 = 0.0352$, $wR_2 = 0.0886$	$R_1 = 0.0431$, $wR_2 = 0.0770$
R indices (all data)	$R_1 = 0.0433$, $wR_2 = 0.0943$	$R_1 = 0.1483$, $wR_2 = 0.0949$
Largest difference peak, hole (e Å^{-3})	0.570, −0.765	0.746, −1.113

3. Results and discussion

3.1. Synthesis of complexes

The reaction of $SnMe_2(OAc)_2$, PLP and valine in 1:1:1 mole ratio in methanol/water (see Section 2 Method A) was carried out with the aim of preparing a complex of $SnMe_2^{2+}$ with the Schiff base derived from the condensation of PLP and the aa, other metal ions having formed complexes of this kind under similar experimental conditions [3]. In the event, the reaction gave [$SnMe_2$(PLP-2H)]·1.5H_2O. Hydrated [$SnMe_2$(PLP-2H)] was also obtained, with a different number of hydration molecules, when $SnMe_2^{2+}$:PLP:valine mole ratios of 1:1:1.5 and 1:2:2 were used. It seems likely that the formation of this complex prevents the formation of, or destabilizes, the Schiff base. The non-hydrated complexes [SnR_2(PLP-2H)] (R = Me, Et, Bu) were prepared by adding solid SnR_2O to a solution of PLP in toluene–ethanol (see Section 2 Method B), which in case of the butyl derivative also avoided hydrolysis of the organometallic cation. All these compounds are solids of poor solubility in most common solvents.

PL, DL-valine and dimethyl- or diethyltin(IV) acetate were reacted in 2:2:1 mole ratio in 80:20 methanol–water at a pH of approximately 6.5 in the hope that the absence of the phosphate group of PLP would prevent the precipitation of PL/SnR_2^{2+} complexes before the formation of the Schiff base between PL and the amino acid. The unexpected formation of complexes **4** and **5** shows that this hope was fulfilled, while at the same time suggesting that formation of the diorganotin(IV) complexes of the Schiff base was followed by expulsion of the ketoacid (probably favored by the presence of the SnR_2^{2+} cation) and condensation of the resulting PM with the excess PL, the final product being a complex of the diorganotin(IV) cation with the deprotonated Schiff base PLPM (see Scheme 3).

The few precedents of the above kind of reaction have led to different products. In discussing the reaction of PL with alanine in the presence of Fe(III), Long et al. [19a] attributed the formation of a dianionic ligand (finally coordinated to the metal) to the prior formation of PLPM and its subsequent reaction with the pyruvic acid produced by the deamination of the alanine; in our work we observed no signs of reaction between PLPM

and the ketoacid afforded by valine. Again, El-Ezaby et al. [19b] hypothesized that certain results obtained in a kinetic study were due to the formation of a complex between Cu(II) and the Schiff base produced by condensation of PLP with pyridoxamine 5′-phosphate; but when a complex of this kind was isolated by Ishida et al. [19c,19d] as the end product of a transamination reaction similar to that described here, it turned out to be a dimer, a covalent bond having been formed between the iminic carbon atoms of two molecules of the Schiff base. In the present study the solids $[SnMe_2(PLPM\text{-}2H)]$ (**4**) and $[SnEt_2(PLPM\text{-}2H)]$ (**5**) were easily isolated by concentration of the crude product of the reaction described above, and their identities and solid-state structures were unequivocally established by X-ray diffractometry (vide infra) following their recrystallization from absolute methanol. Furthermore, exactly the same complexes were obtained when glycine was used instead of valine as the source of the PLPM amino group. However, attempts to obtain the butyl analogue **6** by the same method afforded oils that it was not possible to identify.

It was possible to obtain the butyl analogue **6**- and **4** and **5** and phenyl analogue **7**- by Method B: preparation of PLPM followed by its reaction with the corresponding diorganotin(IV) oxide in 1:1 mole ratio in refluxing 80:20 toluene–ethanol (see Section 2).

3.2. Structures of the complexes in the solid state

In the vibrational spectra of the $[SnR_2(PLP\text{-}2H)]$ species **1**, **2** and **3** the bands associated with the pyridine ring are in positions similar to those they occupy in free PLP, which rules out coordination to the metal via N. By contrast, there are extensive changes between 1100 and 950 cm^{-1}, where the vibrations of the PO_3^{-2} group are found. In this region all three complexes show a pattern compatible [5c,20,21] with a tricoordinating bridging phosphate group giving rise to a polymeric structure similar to that inferred for diorganotin(IV) nucleotide complexes [20], in which the tin atom has distorted octahedral coordination. The non-linearity of the C–Sn–C fragment is shown by the presence of both

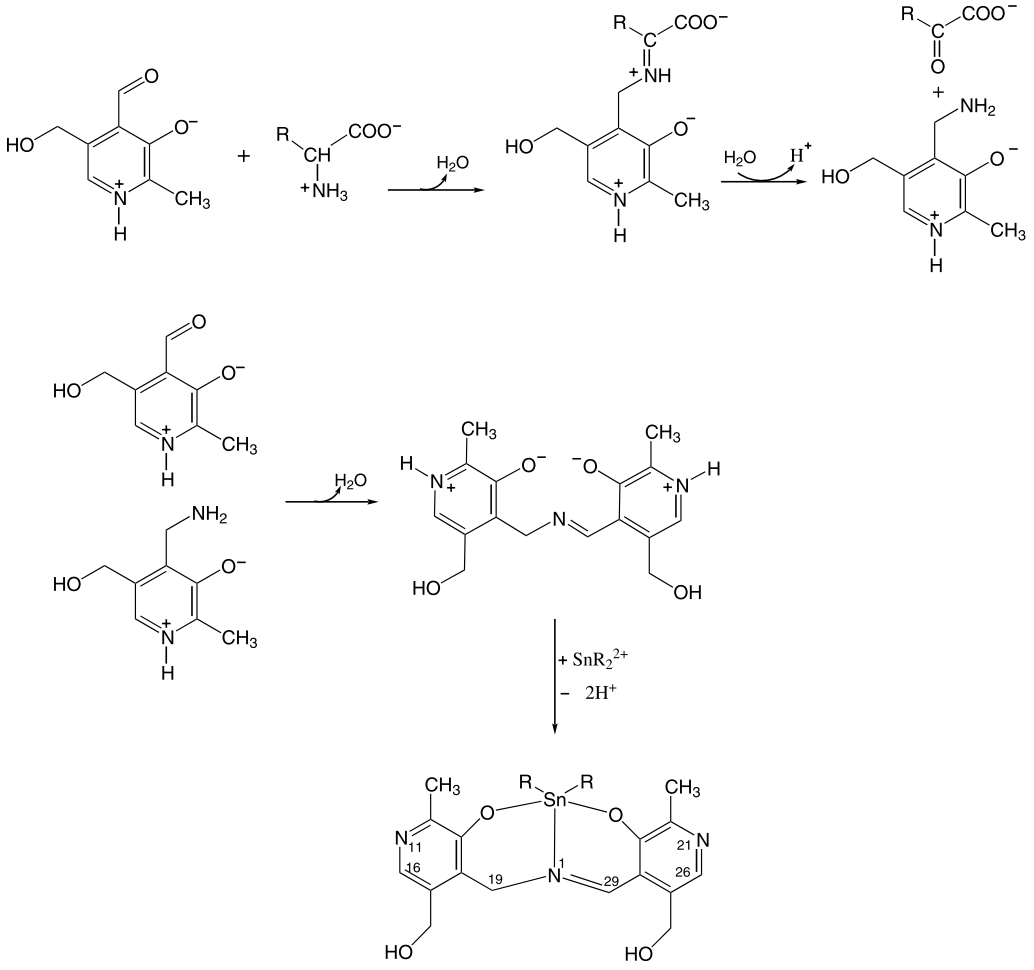

Scheme 3.

ν_{asym}(Sn–C) and ν_{sym}(Sn–C) vibration modes in both IR and Raman spectra.

The Mössbauer spectra of the PLP complexes (see Section 2) consist of well-resolved, slightly asymmetric doublets. The order of their quadrupole splitting values (Me > Et > Bu) is consistent with the hypothesis of a severely distorted octahedral coordination polyhedron with a C–Sn–C bond angle much less than 180°. Point charge calculations give a value of 150° for this angle in the methyl derivative **1** ($Q.S._{calc.} = 3.71$ mm s^{-1}), 140° in **2** ($Q.S._{calc.} = 3.42$ mm s^{-1}) and 135° in **3** ($Q.S._{calc.} = 3.26$ mm s^{-1}).

Thus a polymeric structure based on distorted octahedral tin centers and tricoordinated tetrahedral phosphate groups seems plausible for the poorly soluble complexes **1**, **2** and **3**.

Fig. 1 shows the solid state structure of [$SnMe_2$(PLPM-2H)]·H_2O (**4**·H_2O) together with the numbering scheme used. Selected distances and angles are listed in Table 2. The tridentate ligand coordinates via the two O atoms of the deprotonated phenolic hydroxyl groups and the iminic N atom, so creating two significantly asymmetric six-membered metalacycles. The tin atom is pentacoordinated in a distorted square pyramidal environment (the parameter τ [22], which is 0 for a regular square pyramid and 1 for a trigonal bipyramid, is 0.37), O and C atoms defining the basal plane and the iminic N atom the apex.

The bond lengths in the [PLPM-2H] ligand suggest a charge distribution close to that shown in Scheme 3. The N(1)–C(29) distance corresponds to a double bond, but π density may be delocalized through out the N(1)–C(29)–C(24) fragment, the ring and the C(23)–O(22) bond; this would explain why C(23)–O(22) is shorter than C(13)–O(12) in spite of Sn(1)–O(22) being shorter than Sn(1)–O(12). The two pyridine rings are essentially planar and make a dihedral angle of approximately 70°

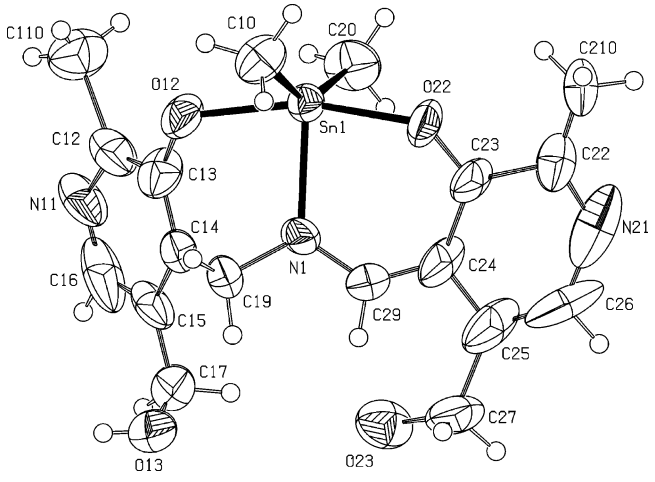

Fig. 1. The crystal structures of [$SnMe_2$(PLPM-2H)]·H_2O (**4**·H_2O), showing the numbering scheme.

Table 2
Bond lengths (Å) and angles (°) in [$SnMe_2$(PLPM-2H)]·H_2O (**4**·H_2O) and [$SnEt_2$(PLPM-2H)] (**5**), with e.s.d's in parentheses

Tin environment	[$SnMe_2$(PLPM-2H)·H_2O (**4** H_2O)	[$SnEt_2$(PLPM-2H)] (**5**)
Sn(1)–C [a]	2.099(7)	2.125(4)
Sn(1)–O(22)	2.100(15)	2.135(3)
Sn(1)–C [b]	2.101(8)	2.138(5)
Sn(1)–O(12)	2.156(18)	2.196(3)
Sn(1)–N(1)	2.202(5)	2.246(3)
C–Sn(1)–O(22)	96.5(9)	91.93(15)
C–Sn(1)–C	142.8(4)	160.64(19)
O(22)–Sn(1)–C	89.2(10)	98.21(18)
C–Sn(1)–O(12)	87.5(9)	88.42(14)
O(22)–Sn(1)–O(12)	164.8(2)	161.76(11)
C–Sn(1)–O(12)	96.5(10)	87.04(16)
C–Sn(1)–N(1)	108.7(3)	100.00(15)
O(22)–Sn(1)–N(1)	82.8(7)	80.88(11)
C–Sn(1)–N(1)	108.5(3)	97.88(17)
O(12)–Sn(1)–N(1)	82.1(7)	81.10(11)
C(13)–O(12)–Sn(1)	121.7(12)	120.5(2)
C(23)–O(22)–Sn(1)	124.3(13)	125.4(3)
C(29)–N(1)–Sn(1)	122.0(9)	125.8(3)
C(19)–N(1)–Sn(1)	120.5(9)	117.3(3)
C(2)–C(1)–Sn(1)		122.1(4)
C(4)–C(3)–Sn(1)		114.9(3)
Pyridoxal-pyridoxamine ligand		
O(12)–C(13)	1.37(2)	1.346(5)
O(22)–C(23)	1.29(2)	1.326(5)
O(13)–C(17)	1.394(17)	1.422(6)
O(23)–C(27)	1.413(15)	1.399(5)
N(1)–C(29)	1.343(17)	1.265(5)
N(1)–C(19)	1.420(16)	1.490(5)
N(11)–C(16)	1.29(4)	1.341(6)
N(11)–C(12)	1.39(2)	1.332(5)
N(21)–C(22)	1.32(3)	1.335(5)
N(21)–C(26)	1.39(4)	1.341(5)
C(13)–C(14)	1.33(3)	1.401(5)
C(13)–C(12)	1.34(3)	1.412(6)
C(12)–C(110)	1.75(3)	1.496(6)
C(16)–C(15)	1.40(4)	1.379(6)
C(15)–C(14)	1.42(3)	1.400(6)
C(15)–C(17)	1.43(2)	1.500(6)
C(14)–C(19)	1.73(3)	1.511(6)
C(23)–C(24)	1.45(3)	1.405(5)
C(23)–C(22)	1.46(3)	1.418(5)
C(22)–C(210)	1.32(3)	1.494(6)
C(26)–C(25)	1.30(4)	1.368(6)
C(25)–C(24)	1.40(3)	1.411(6)
C(25)–C(27)	1.59(3)	1.523(6)
C(24)–C(29)	1.26(2)	1.475(6)
C(1)–C(2)		1.472(7)
C(3)–C(4)		1.516(6)
C(29)–N(1)–C(19)	117.5(6)	116.8(4)
C(16)–N(11)–C(12)	111(2)	118.8(4)
C(22)–N(21)–C(26)	126(2)	118.9(4)
C(14)–C(13)–C(12)	116.8(19)	119.1(4)
C(14)–C(13)–O(12)	123(2)	120.3(4)
C(12)–C(13)–O(12)	120.5(17)	120.7(4)
C(13)–C(12)–N(11)	130(2)	121.1(4)
C(13)–C(12)–C(110)	124.4(17)	121.4(4)
N(11)–C(12)–C(110)	106(2)	117.4(4)
N(11)–C(16)–C(15)	125.5(17)	124.8(4)
C(16)–C(15)–C(14)	118(2)	117.0(4)

Table 2 (*Continued*)

Tin environment	$[SnMe_2(PLPM\text{-}2H)\cdot H_2O$ (**4** H_2O)	$[SnEt_2(PLPM\text{-}2H)]$ (**5**)
C(16)–C(15)–C(17)	110.4(18)	120.0(4)
C(14)–C(15)–C(17)	131(2)	123.0(4)
C(13)–C(14)–C(15)	118(2)	119.2(4)
C(13)–C(14)–C(19)	114.8(18)	117.0(4)
C(15)–C(14)–C(19)	126.6(18)	123.8(4)
N(1)–C(19)–C(14)	105.0(10)	108.2(4)
O(22)–C(23)–C(24)	121.6(19)	123.2(4)
O(22)–C(23)–C(22)	119.3(18)	118.6(4)
C(24)–C(23)–C(22)	119.1(17)	118.1(4)
C(210)–C(22)–N(21)	130(2)	118.3(4)
C(210)–C(22)–C(23)	117.2(18)	120.1(4)
N(21)–C(22)–C(23)	112(2)	121.7(4)
C(25)–C(26)–N(21)	126(2)	124.2(4)
C(26)–C(25)–C(24)	113(2)	117.8(4)
C(26)–C(25)–C(27)	127.2(19)	118.7(4)
C(24)–C(25)–C(27)	119(2)	123.5(4)
C(29)–C(24)–C(25)	111(2)	118.8(4)
C(29)–C(24)–C(23)	125.4(17)	122.3(4)
C(25)–C(24)–C(23)	123(2)	118.8(4)
C(24)–C(29)–N(1)	130.3(12)	125.3(4)
O(13)–C(17)–C(15)	106.5(15)	114.2(4)
O(23)–C(27)–C(25)	115.0(10)	115.7(4)

[a] C(10) for **4**·H_2O and C(3) for **5**.
[b] C(20) for **4**·H_2O and C(1) for **5**.

with each other. Roughly, the molecule is like a half open book with the N(1)–Sn(1) bond as its spine, the pyridine rings as pages, and the methyl groups bound to the tin atom as page-marking ribbons.

The $[SnMe_2(PLPM\text{-}2H)]$ molecules form hydrogen bonds, some of which also involve the molecule of water of crystallization. Specifically O(13)–H(13) interacts with the O(22) atom of a neighboring molecule [0.82, 2.29 and 2.969(19) Å; 140.0°]; O(23)–H(23) interacts with the O^{i} atom of H_2O^{i} [0.82, 2.31 and 2.874(12) Å; 126.7°; i = $-x+1$; $y+1/2$, $-z+2$]; one of the hydrogen

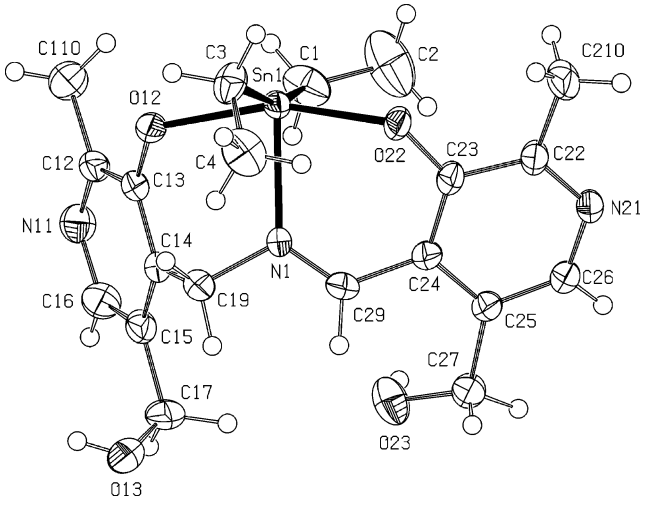

Fig. 2. The crystal structures of $[SnEt_2(PLPM\text{-}2H)]$ (**5**), showing the numbering scheme.

atoms of the water molecule [H(1B)] is bound to $N(11)^{ii}$ [0.91, 2.14 and 2.81(2) Å; 130.2°; ii = $-x$; $y-1/2$, $-z+2$]; and the other, [H(1A)], is bound to $N(21)^{iii}$ [1.25, 1.86 and 2.83(3) Å; 128.2°; iii = x; $y+1$, z].

Fig. 2 shows the structure of $[SnEt_2(PLPM\text{-}2H)]$ (**5**) with the numbering scheme used. Selected distances and angles are listed in Table 2. In this compound the coordination mode of the ligand is similar to that described above for **4**·H_2O but, probably due to steric hidrance, the Sn–N(1), Sn–O(22) and Sn–O(12) distances are longer than in the latter [2.246(3), 2.135(3) 2.196(3) Å as against 2.202(5), 2.100(15) and 2.156(18) Å, respectively]. The coordination polyhedron of the tin atom is again square-pyramidal, but O(22)–Sn–O(12) [161.76(11)°] is slightly narrower and C–Sn–C [160.64 (19)°] rather wider than in **4**·H_2O [164.8(2)° and 142.8 (4)°, respectively], which makes the base of the pyramid- and the pyramid as a whole- more regular ($\tau = 0.02$) [22].

The C(29)–N(1)–C(19) fragment of the PLPM-2H ligand shows the difference between the two C–N bonds even more clearly than in **4**·H_2O. The ligands of the two compounds also appear to differ as regards other structural parameters, but the large e.s.d. values for **4**·H_2O preclude detailed comparison. The two pyridine rings are again essentially planar, and in this case make a dihedral angle of approximately 71.7°.

The only hydrogen bond in **5** involves the O(23)–H(23) group and one of the pyridine N atoms of a neighboring molecule, $N(11)^{i}$ [0.91, 1.92 and 2.736(5)Å; 148°; i = $-x+1/2$; $-y+3/2$, $-z$].

Table 3 compares the most significant structural parameters of the tin coordination sphere in **4**·H_2O and **5** with those of pentacoordinate complexes containing similar N,O,O-donor ligands. In all these complexes the Sn–C and Sn–O bond lengths are similar, but the Sn–N bond of **5** is longer than that of any other compound listed in the table. Also, the O–Sn–O and C–Sn–C angles of **4**·H_2O and **5** are wider than those of the other complexes.

The IR and Raman spectra of PLPM and its complexes were interpreted on the basis of previous work on other Schiff bases and related complexes [28–33]. In the 3400–3000 cm^{-1} region the spectrum of the free ligand has strong, broad bands that can be attributed to ν(OH) of the CH_2OH group and to either ν(OH) of the phenolic hydroxyl or $\nu(NH^{+})$ of the protonated pyridine rings (see Scheme 3). This part of the spectrum of PLPM is significantly simplified by deprotonation and coordination to the metal, which also shift the strong $\nu(C\text{–}O_{phenolic})$ band at 1286 cm^{-1} to higher wavenumbers and the ν(C–N) band from 1634 to 1625 ± 6 cm^{-1}. These shifts are similar in all four PLPM complexes, suggesting that the coordination mode of the ligand is the same in all four.

The Mössbauer spectra suggest that there are nevertheless certain structural differences between the PLPM-

Table 3
Comparison of relevant structural parameters of similar pentacoordinate dimethyl– and diethyltin(IV) compounds with those of **4**·H_2O and **5**

Compound	Sn–C	Sn–O	Sn–N	O–Sn–O	C–Sn–C	Ref.
$[SnMe_2(OC_6H_4CH{=}NC_6H_4O)]$	2.10(1); 2.12(1)	2.108(6); 2.130(7)	2.225(8)	158.5	139.6(4)	[23]
$[SnMe_2(OC_6H_4CH{=}NC_6H_4O)]$	2.091(14); 2.142(14)	2.118(9); 2.105(8)	2.229(11)	158.58(35)	138.6(50)	[24]
$[SnMe_2(O(t\text{-}Bu)_2C_6H_2NC_6H_2O(t\text{-}Bu)_2O)]$	2.083(6); 2.099(6)	2.111(4); 2.115(4)	2.146(4)	151.6(1)	125.9(3)	[25]
$[(SnMe_2)_2(O(t\text{-}Bu_2)C_6H_2NCO)_2]$	2.104(5); 2.102(5)	2.059(3); 2.210(3)	2.133(3)	151.40(11)	127.97(19)	[26]
4·H_2O	2.099(7); 2.101(8)	2.100(15); 2.156(18)	2.202(5)	164.8(2)	142.8(4)	This work
$[(SnEt_2)_2(OC_6H_4CH{=}NNCO)_2CH_2]$	2.119(8); 2.102(9)	2.098(6); 2.193(6)	2.206(6)	153.3(2)	135.5(3)	[27]
5	2.125(4); 2.138(5)	2.135(3); 2.196(3)	2.246(3)	161.76(11)	160.64(19)	This work

2H complexes with the smaller organic groups (R = Me, Et) and those with the bigger ones (R = Bu, Ph) the isomer shifts and quadrupole splitting values being clearly larger in the former [I.S. (mm s^{-1}) = 1.45 (Me), 1.54 (Et); Q.S. (mm s^{-1}) = 3.64 (Me), 3.63 (Et)] than in the latter [I.S. (mm s^{-1}) = 1.38 (Bu), 1.17 (Ph); Q.S. (mm s^{-1}) = 2.87 (Bu), 2.58 (Ph)].

Given that all four have the same coordination mode (vide supra), it seems probable that these spectral differences derive from a change in the C–Sn–C bond angle, which may be narrower in the Bu and Ph complexes due to steric and/or electronic factors. In $[SnPh_2(L)]$ (L^{2-} = salicylaldehydethiosemicarbazonato), pentacoordinate tin complex containing an N,O,S-bonded instead of an N,O,O-bonded ligand, the very narrow C–Sn–C bond angle [127.0(2)°] is also associated with very low I.S. and Q.S. values (1.30 and 2.30 mm s^{-1}, respectively) [34].

The ^{13}C CP MAS spectra of PLPM, **4** and **5** were recorded using polycrystalline samples and were interpreted in accordance with the information obtained in solution (vide infra) and in previous studies of similar compounds [5a,5b]. The observed deshielding of C(29), C(19), C(23) and C(13) upon formation of the complexes is in keeping with the N(1),O(12),O(22)-coordination established by X ray diffractometry. The fact that the very well resolved spectrum of **5** (Fig. 3) shows two signals for the methyl groups of the $SnEt_2$ moiety is probably due to their different orientations with respect to the ligand: one of these groups [–C(4)H_3] lies almost in the plane defined by the N(1)–Sn–C(3) fragment while the other [–C(2)H_3] is close to the plane of the O(22), Sn and C(1) atoms (Fig. 2).

3.3. Structures of the complexes in solution

Assignation of the proton NMR signals of PLPM was initially carried out on the basis of the data for pyridoxine [5a] [35] and was subsequently confirmed by DEPT and heteronuclear correlation experiments (HMBC and HMQC), which also allowed interpretation of the ^{13}C NMR spectrum. Only one of the two protons that are lost upon formation of $(PLPM\text{-}2H)^{2-}$ was located, as a broad singlet at 14.26 ppm. The azomethine proton appeared as a singlet at 9.01 ppm.

In the spectra of the complexes the low field signal is absent, in keeping with the deprotonation of the ligand. Coordination slightly shifts most ligand proton signals to higher field, and the fact that the greatest shifts affect H(16) and H(26) suggests that deprotonation occurs at N(11) and N(21) (see Fig. 1). Of particular significance for identifying the coordination mode of the ligand is the signal of the azomethine proton [H(29)], which in the spectra of all the complexes is flanked by a pair of

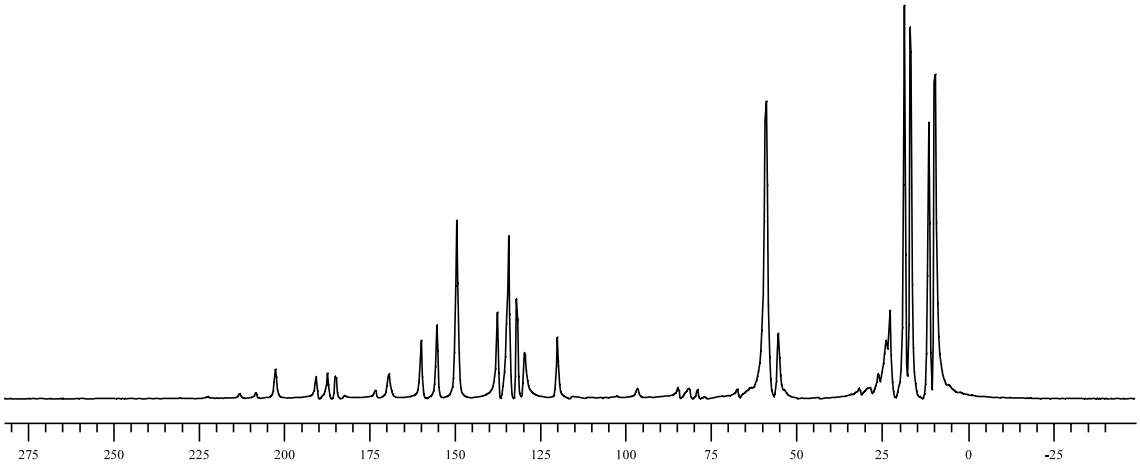

Fig. 3. ^{13}C CP MAS NMR spectrum of $[SnEt_2(PLPM\text{-}2H)]$ (**5**).

satellites due to coupling with the tin atom [$^3J(^1H-^{119}Sn) = 26$, 25, 36 and 52 Hz for **4**, **5**, **6** and **7**, respectively]; this is a clear indication that the N(1) atom remains coordinated to the metal in dmso-d_6 solution. In the spectrum of the diphenyltin complex this coupling also affects the H(19) signal.

The ^1H NMR signal of the dimethyl-tin group of **4**·H_2O is a singlet at 0.5 ppm with two satellites [$^2J(^1H-^{119}Sn) = 95.9$ Hz]. Substitution of the coupling constant in the Lockhart–Manders equation [36] gives a value of 155° for the C–Sn–C angle. This is wider than in the solid state (142.8°), and may indicate interaction of the metal with dmso-d_6.

The ^{13}C NMR signals of the ligand in **4** and **5** are located at positions very close to those observed in the solid state, showing that the coordination mode of PLPM-2H in the solid state persists in solution in dmso-d_6. In the spectrum of [$SnMe_2$(PLPM-2H)]·H_2O the signal of the $SnMe_2$ moiety is flanked by satellites indicative of coupling between the ^{13}C and the $^{119/117}Sn$ nuclides. When the coupling constant [$^1J(^{13}C-^{119/117}Sn) = 910.4/869.6$ Hz] is substituted in the corresponding Lockhart–Manders equation [36], a value of 157° is obtained for the angle C–Sn–C in close agreement with that derived from $^2J(^1H-^{119}Sn)$.

The ^{119}Sn NMR spectra of the complexes [$SnMe_2$(PLPM-2H)]·H_2O, [$SnBu_2$(PLPM-2H)] and [$SnPh_2$(PLPM-2H)] each show just one signal (at −305.8, −285.0 and −485.9 ppm, respectively), while the spectrum of the ethyl complex [$SnEt_2$(PLPM-2H)] shows two, at −326.6 and −330.2 ppm. Although $\delta(^{119}Sn)$ is influenced by several factors, including the aromatic or aliphatic nature of the group R bound to the tin atom (and possibly the type of donor atoms of the ligand [34]), it may be used with caution to infer the coordination number of the tin atom [37]. In the case of Sn^nBu_2 (IV) compounds different coordination numbers are clearly associated with different ranges of $\delta(^{119}Sn)$ values, and the chemical schift of [$SnBu_2$(PLPM-2H)] is well within the range corresponding to coordination number 6, −210 to −400 ppm [37b]. Similarly, the chemical shift of [$SnPh_2$(PLPM-2H)] is in the range characteristic of hexacoordinate diphenyltin(IV) compounds, −360 to −540 ppm [37b]. Like the methyl complex (vide supra), the butyl and phenyl complexes may include a dmso molecule in the coordination sphere of the metal when dissolved in this solvent. The presence of two signals very close to each other in the spectrum of the diethyltin(IV) derivative may be due to the existence of two types of molecule with slightly different orientations of their Et groups.

3.4. Antibacterial activity

All the complexes had detectable activities against the five bacterial strains assayed (Table 4), those of the Bu and Ph derivatives—especially the former—generally being slightly greater than those of their Me and Et analogues. This is in keeping with previous reports on the activity of butyl and phenyl organotin compounds [38]. The superiority of the Bu and Ph compounds was especially evident with the more sensitive Gram-(+) bacteria, especially *B. subtilis*, in concordance with previous reports [39].

Despite the reported antibacterial activity of various Schiff bases [40] and the alleged role of PL and PM as cofactors of enzymes targeted by certain antimicrobials [41,42], PLPM did not show any detectable antibacterial activity against four of the five strains assayed. It was nevertheless strongly active against *P. aeruginosa* (ATCC27853), a bacteria belonging to a genus previously reported to be sensitive to other Schiff bases [43]. By contrast, the carbapenem-resistant clinical isolate of *P. aeruginosa* showed no sensitivity to PLPM. Since resistance to carbapenems is usually associated with changes in permeability [44], it seems possible that one of the effects of coordination to Sn may be to facilitate the penetration of PLPM via an alternative transport route.

4. Supplementary data

Crystallographic data have been deposited with The Director, CCDC, 12, Union Road, Cambridge, CB2 1EZ, UK (fax: +44-1223-366033; e-mail: deposit@ccdc.cam.ac.uk or www: http://www.ccdc.cam.uk) and are available on request, quoting the deposition number 188539 and 188540 for **4**·H_2O and **5**, respectively.

Table 4
Antibacterial activities of PLPM and its complexes[a]

Organism	PLPM	**4**·H_2O	**5**	**6**	**7**
E. coli	> 250	62.5	62.5	31.25	15.62
S. aureus	> 250	125	125	15.62	15.62
B. subtilis	> 250	62.5	31.25	3.9	15.62
P. aeruginosa ATCC27853	< 1.95	< 1.95	< 1.95	< 1.95	< 1.95
Carbapenem-resistant *P. aeruginosa*	> 250	31.25	15.62	15.62	31.25

[a] Minimum inhibitory concentration (MIC).

Acknowledgements

We thank the Xunta de Galicia, Spain, for financial support under Project XUGA 20316 B94. F. Condori thanks the Spanish Agency for International Cooperation and the University of Santiago de Compostela for grants.

References

[1] R.A. John, Biochim. Biophys. Acta 1248 (1995) 81.
[2] R.F. Zabinski, M.D. Toney, J. Am. Chem. Soc. 123 (2001) 193 (and references therein).
[3] (a) G.A. Bentley, J.M. Waters, T.N. Waters, Chem. Commun. (1968) 988;
(b) S.P. Sudhakara Rao, H. Manohar, J. Chem. Soc., Dalton Trans. (1985) 2051;
(c) I. Mathews, H. Manohar, J. Chem. Soc., Dalton Trans. (1991) 2289;
(d) I.I. Mathews, H. Manohar, Polyhedrom 10 (1991) 2163.
[4] (a) N. Christensen, J. Am. Chem. Soc. 77 (1955) 2431;
(b) S. Yamada, Y. Kuge, T. Yamayoshi, Inorg. Chim. Acta 8 (1974) 29;
(c) T. Wrobleski, G.J. Long, Inorg. Chem. 16 (1977) 2752;
(d) T. Wrobleski, G.J. Long, Inorg. Chim. Acta 36 (1979) 155;
(e) E. Willstadter, T.A. Hamor, J.L. Hoard, J. Am. Chem. Soc. 85 (1963) 1205;
(f) J.F. Cutfield, D. Hall, T.N. Waters, Chem. Commun. (1967) 785;
(g) H.M. Dawes, J.M. Waters, T.N. Waters, Inorg. Chim. Acta 66 (1982) 29;
(h) S. Capasso, F. Giordano, C. Mattia, L. Mazzarella, A. Ripamonti, J. Chem. Soc., Dalton Trans. (1973) 2228;
(i) S.P. Sudhakara Rao, H. Manohar, J. Chem. Soc., Dalton Trans. (1985) 2051;
(j) I. Mathews, H. Manohar, J. Chem. Soc., Dalton Trans. (1991) 2289;
(k) G.J. Long, J.T. Wrobleski, R.V. Thundathil, D.M. Sporlin, E.O. Schlemper, J. Am. Chem. Soc. 102 (1980) 6040;
(l) K. Aoki, H. Yamazaki, J. Chem. Soc., Chem. Commun. (1980) 363;
(m) D.L. Leussing, N. Huq, Anal. Chem. 38 (1966) 1388;
(n) Y. Matsushima, Chem. Pharm. Bull. 16 (1968) 2143;
(o) H. Abbott, A.E. Martell, J. Am. Chem. Soc. (1970) 5845;
(p) E.H. Abbott, J. Inorg. Nucl. Chem. 33 (1971) 567;
(q) E.H. Abbott, A.E. Martell, J. Am. Chem. Soc. (1973) 5014;
(r) L. Casella, M. Gullotti, G. Pacchioni, J. Am. Chem. Soc. 104 (1982) 2386;
(s) V.M. Shanbhag, A.E. Martell, Inorg. Chem. 29 (1990) 1023;
(t) W.L. Felty, D.L. Leussing, J. Inorg. Nucl. Chem. 36 (1974) 617;
(u) L.M. Wis Vitolo, G.T. Hefter, B.W. Clare, J. Webb, Inorg. Chim. Acta 170 (1990) 171.
[5] (a) J.S. Casas, E.E. Castellano, F. Condori, M.D. Couce, A. Sánchez, J. Sordo, J.M. Varela, J. Zuckerman-Schpector, J. Chem. Soc., Dalton Trans. (1997) 4421;
(b) J.S. Casas, A. Castiñeiras, F. Condori, M.D. Couce, U. Russo, A. Sánchez, J. Sordo, J.M. Varela, Polyhedron 19 (2000) 813;
(c) J.S. Casas, E.E. Castellano, M.D. Couce, M.S. García-Tasende, A. Sánchez, J. Sordo, C. Taboada, E.M. Vázquez-López, Inorg. Chem. 40 (2001) 946.
[6] M. Nath, S. Goyal, Main Group Met. Chem. 19 (1996) 75.
[7] (a) M. Nath, R. Yadav, M. Gielen, H. Dalil, D. Vos, G. Eng, Appl. Organomet. Chem. 11 (1997) 727;
(b) M.B. Ferrari, G.G. Fava, C. Pelizzi, G. Pelosi, P. Tarasconi, Inorg. Chim. Acta 269 (1998) 297;
(c) J.S. Casas, M.C. Rodríguez-Argüelles, U. Russo, A. Sánchez, J. Sordo, A. Vázquez-López, S. Pinelli, P. Lunghi, A. Bonati, R. Albertini, J. Inorg. Biochem. 69 (1998) 283.
[8] R.S. Tobias, I. Ogrins, B.A. Nevett, Inorg. Chem. 1 (1962) 636.
[9] H.N. Christensen, J. Am. Chem. Soc 79 (1957) 4073.
[10] C.L. Mac Laurin, M.F. Richardson, Acta Crystallogr. C41 (1985) 261.
[11] B.V. Nonius, CAD4-EXPRESS Software, Versión 5.1/1.2, Enraf-Nonius, Delft, The Netherlands, 1994.
[12] M. Kretschmar, GENHKL, Program for the Reduction of CAD4 diffractometer data, University of Tuebingen, Germany, 1997.
[13] C.T. North, D.C. Phillips, F.S. Mathews, Acta Crystallogr. A24 (1968) 351.
[14] G.M. Sheldrick, Acta Crystallogr. A46 (1990) 467.
[15] G.M. Shelrick, SHELXL-97, Program for the Refinement of Crystal Structures, University of Goettingen, Germany, 1997.
[16] H.D. Flack, Acta Crystallogr. A39 (1983) 876.
[17] International Tables for X-ray Crystallography, vol. C, Kluwer Academic Publishers, Dordrecht, The Netherlands, 1995.
[18] L. Spek, Acta Crystallogr. A46 (1990) C34.
[19a] G.J. Long, J.T. Wrobleski, R.V. Thundathil, D.M. Sparlin, E.O. Schlemper, J. Am. Chem. Soc. 102 (1980) 6040.
[19b] H.M. Marafie, M.S. El-Ezaby, S. Fareed, J. Inorg. Biochem. 37 (1989) 7.
[19c] T. Ishida, Y. In, C. Hayashi, R. Manabe, A. Wakahara, Bull. Chem. Soc. Jpn. 70 (1997) 2375.
[19d] T. Ishida, R. Manabe, Y. In, H. Takashima, K. Kitamura, A. Wakahara, Bull. Chem. Soc. Jpn. 72 (1999) 947.
[20] Q. Li, P. Yang, E. Hua, C. Tian, J. Coord. Chem. 40 (1996) 227.
[21] M.E. Farago, M.M. McMillan, S.S. Sabir, Inorg. Chim. Acta 14 (1975) 207.
[22] A.W. Addison, T. Nageswara Rao, J. Reedijk, J. Van Rijn, G.C. Verschoov, J. Chem. Soc., Dalton Trans. (1984) 1349.
[23] D.L. Evans, B.L. Penfold, J. Cryst. Mol. Struct. 5 (1975) 93.
[24] H. Preut, F. Huber, H.J. Haupt, R. Cefalu, R. Barbieri, Z. Anorg. Allg. Chem. 410 (1974) 88.
[25] C. Camacho-Camacho, H. Tlahuext, H. Nötha, R. Contreras, Heteroatom Chem. 9 (1998) 321.
[26] R. Contreras, V.M. Jimenez-Perez, C. Camacho-Camacho, M. Guisado-Rodriguez, B. Wrackmeyer, J. Organomet. Chem. 604 (2000) 229.
[27] M.P. Degaonkar, V.G. Puranik, S.S. Tavale, S. Gopinathan, C. Gopinathan, Bull. Chem. Soc. Jpn. 67 (1994) 1797.
[28] N.A. Drobinskaya, I.V. Inova, M. ya. Karpeiskii, V.L. Florent'ev, Chem. Heterocycl. Compd. 7 (1973) 330 (Engl. Trans.).
[29] J.N.R. Ruddick, J.R. Sams, J. Organomet. Chem. 60 (1973) 233.
[30] N.S. Biradar, N.H. Kulkarni, J. Inorg. Nucl. Chem. 33 (1971) 245.
[31] M.J. Benecky, R.A. Copeland, T.R. Hays, E.W. Lobenstine, R.P. Rava, Jr., R.A. Pascal, T.G. Spiro, J. Biol. Chem. 260 (1984) 11663.
[32] D.K. Dey, M.K. Das, H. Nöth, Z. Naturforsch 54b (1999) 145.
[33] D. Kumar Dey, M. Kumar Saha, M. Kanti Das, N. Bhartiya, R.K. Bansal, G. Rosair, S. Mitra, Polyhedron 18 (1999) 2687.
[34] J.S. Casas, A. Sánchez, J. Sordo, A. Vázquez-López, E.E. Castellano, J. Zukerman-Schpector, M.C. Rodríguez-Argüelles, U. Ruso, Inorg. Chim. Acta 216 (1994) 169.
[35] (a) F. Kayser, M. Biesemans, M. Gielen, R. Willem, Main Group Met. Chem. 17 (1994) 559;
(b) F. Kayser, M. Biesemans, M. Gielen, R. Willem, Magn. Reson. Chem. 32 (1994) 358.
[36] T.P. Lockhart, W.F. Manders, Inorg. Chem. 25 (1986) 892.
[37] (a) J. Otera, J. Organomet. Chem. 221 (1981) 57;
(b) J. Holocek, A. Lycka, K. Handlír, M. Nádvorník, Collect. Czech. Chem. Commun. 55 (1990) 1193.

[38] M. Nath, R. Yadav, Bull. Chem. Soc. Jpn. 70 (1997) 1331.
[39] J. .S. Casas, E. García Martínez, M.L. Jorge, U. Russo, A. Sánchez, A. Sánchez González, R. Seoane, J. Sordo, Appl. Organomet. Chem. 15 (2001) 204.
[40] H.L. Singh, S. Varshney, A.K. Varshney, Appl. Organomet. Chem. 14 (2000) 212.
[41] P.W. Van Ophem, D. Peisach, S.D. Erickson, K. Soda, D. Ringe, J.M. Manning, Biochemistry 38 (1999) 1323.
[42] R. Contestabile, T.L. Jenn, M. Akhtar, D. Gani, R.A. Jonh, Biochemistry 39 (2000) 3091.
[43] H.L. Singh, S. Varshney, K. Varshney, Appl. Organomet. Chem. 14 (1999) 212.
[44] Y. Sumita, M. Fukasawa, Chemotherapy 42 (1996) 47.